

Experimental and finite element analyses of footings of varying shapes on sand

Özgür Anil^{*}, S. Oğuzhan Akbaş^a, Salih Babagiray^b,
A. Cem Gel^c and Cengizhan Durucan^d

Civil Engineering Department, Gazi University, Maltepe, Ankara 06570, Turkey

(Received January 29, 2015, Revised October 01, 2016, Accepted October 20, 2016)

Abstract. In this study, bearing capacities and settlement profiles of six irregularly shaped footings located on sand have been experimentally and analytically investigated under the effect of axial loading. The main variable considered in the study was the geometry of the footings. The axial loads were applied from the center of gravities of the test specimens. Consequently, the effect of footing shape on the variation of the bearing capacities and settlement profiles have been investigated in this paper. The three dimensional finite element analyses of the test specimens were conducted using the PLAXIS 3D software. The finite element model results are in acceptable agreement with the results obtained using experimental investigation. In addition, the usability of the finite element technique by design engineers to determine the bearing capacities and settlement profiles of irregularly shaped footings was investigated. From the results of the study, it was observed that the geometric properties of the footings significantly influenced the variation of the bearing capacities and settlement profiles.

Keywords: bearing capacity of foundation; shape factor; settlement profile; finite element analysis; geometry of footing

1. Introduction

The bearing capacities and settlement profiles of the footings are important parameters that significantly affect the safety and usability of structures. Also, it is a widely known fact that the foundation design is function of safety and usability of structures by means of transfer of the loads from the superstructure and the stability of the structure. On the other hand, satisfying the bearing capacity requirements of the footings is not sufficient alone to obtain a safe foundation design. In addition, the settlement profile of a footing is an important factor which seriously affects the structures and may lead to damage that may have serious influence on the performance of the superstructure. Strength and stability of structures can be seriously affected by distortion of the structure resulting from differential settlements of the footings. Consequently, a foundation design providing an equal settlement under the design loads for all the footings is commonly targeted

*Corresponding author, Ph.D., Professor, E-mail: oanil@gazi.edu.tr

^a Professor, E-mail: soakbas@gazi.edu.tr

^b M.Sc., E-mail: salihbabagiray@gmail.com

^c Ph.D., E-mail: ahmetcem.gel@gazi.edu.tr

^d Ph.D., E-mail: cengizhandurucan@gmail.com

engineering approach to prevent damage to superstructures.

However, in some cases, the footings may have irregular shapes due to the geometry of the structure and architectural concerns. Effects of such irregular footing geometries on the variation of settlement profiles and bearing capacities are important research topics. Consequently, the bearing capacities of foundations have always been a subject of major interest in soil mechanics, structural and foundation engineering. Most of the design methods proposed to estimate the bearing capacity are based on the original studies of Prandtl (1921), Reissner (1924) and Terzaghi (1943). In some studies the method proposed by Prandtl (1921) and Reissner (1924) have been modified to accommodate the conditions not included in the Prandtl-Reissner solution, such as load inclination and footing shape. Similar to these studies, the bearing capacity equation developed by Terzaghi, 1943 is one tool that is frequently used by geotechnical engineers. It is used to estimate the limit unit load (referred to also as the limit unit bearing capacity or limit unit base resistance) that will cause a footing to undergo bearing capacity failure (Terzaghi 1943, Meyerhof 1951, 1963, Hansen 1970).

In the literature there are numerous studies focusing on both the theoretical and experimental aspects of bearing capacities of foundations. A list of some comprehensive contributions to the subject may be found in Vesic (1975), Chen and McCarron (1991) and Tani and Craig (1995). Furthermore, more recent studies focused on the bearing capacities of footings are summarized below.

Shahin and Cheung (2011), estimated the probable distribution of predicted bearing capacities of strip footings subjected to vertical loads using a stochastic approach based on the Monte Carlo simulation. Mohamed *et al.* (2013), proposed simple relationships for the settlement estimations of square footings carrying vertical loads in saturated and unsaturated sandy soils. In the study, seven large-scale footings tested under both saturated and unsaturated conditions were used to validate the proposed technique. In study conducted by Dixit and Patil (2013), test results, in terms of bearing capacities, of square footings resting on sand were presented and compared with the available analytical equations. Naderi and Hata (2014), numerically and experimentally investigated the bearing capacities of closely located ring and circular footings on reinforced sand. Furthermore, the effect of interference on the bearing capacities of adjacent circular and ring footings were evaluated. Similarly, in a study conducted by Mabrouki *et al.* (2010), the bearing capacities of two interfering strip footings, subjected to centered vertical loads with smooth and rough interfaces were evaluated.

From the literature review, it was observed that the bearing capacity equations are proposed based on the investigation of foundations having regular shapes such as, square, circle, ring and rectangle. It was also observed that the effects of varying diameter lengths and varying width to length ratios on the variation of bearing capacities and settlement profiles of the footings were investigated for circular and rectangular foundations, respectively (Lyamin *et al.* 2007, De Beer 1970, Mabrouki *et al.* 2009, Zhu and Michalowski 2005). However, in the literature no study was found on understanding the behavior of irregularly shaped, i.e., hollow square, U shaped or L shaped foundations. Consequently, the experimental and finite element analyses of such irregularly shaped foundations under axial loads were performed in this paper.

For this purpose, firstly, the bearing capacities and settlement profiles of six irregularly shaped footings located on sand have been experimentally investigated. In the study the main variable was the geometry of the footing. The bearing capacities and settlement profiles of these irregularly shaped footings are obtained and comparatively presented with those of a regular square footing having the dimensions of 400 mm × 400 mm. First, axial loading tests on two hollow square

footings, each having one opening with the dimensions of 100 mm × 100 mm and 200 mm × 200 mm, were conducted. Then, U-shaped and two different L-shaped footings were tested and the results comparatively presented. After obtaining the results of the experimental study, 3-D finite element analyses of the test specimens were performed using the PLAXIS 3D software. Based on that, an analytical model was obtained to help the foundation design engineers.

2. Experimental study

2.1 Test specimen and materials

In the scope of the experimental phase of the study, six specimens were tested. The geometric configurations and the dimensions of the test specimens are presented in Table 1 and Fig. 1, respectively. The footing shape is the investigated variable in the experimental phase of the study. In the experimental study, the square shaped footing with the dimensions of 400 mm × 400 mm was used as reference specimen to comparatively interpret the effect of footing shape irregularity on the bearing capacities and settlement profiles of the footings. Then, five irregularly shaped specimens were tested and load – settlement relationships were obtained. In the experimental study, all of the test specimens had a maximum side length of 400 mm and were able to be fitted within a square of dimensions 400 mm × 400 mm. On the other hand, all test specimens have several irregularities in shape. Test specimen – 2 have a square opening of dimensions 200 mm × 200 mm located at the intersection of the symmetry axes. Similarly, test specimen - 3 have a square opening of dimensions 100 mm × 100 mm located at the intersection of the symmetry axes. Test specimen – 4 was manufactured in the shape of an *L*. Test specimen – 5 was manufactured in the shape of a *U* and test specimen – 6 was manufactured in a shape of *L* similar to test specimen – 4. However, in this case the legs of *L* were a little thinner than the legs of the test specimen – 4.

The test specimens are designed to have irregular shapes with openings that vary in size and location within the footing. The opening of dimensions 200 mm × 200 mm located at the center of the symmetry in test specimen – 2. The dimensions of this opening was reduced to 100 mm × 100 mm and located at the center of test specimen – 3. In test specimens 4 and 5 the square opening in the dimensions of 200 mm × 200 mm was used in different locations and in the test specimen – 6 the location of the opening was changed together with the increased dimensions (i.e., 250 mm × 250 mm) of the opening.

In the experimental study, all of the test specimens were manufactured using high strength steel to represent a rigid foundation behavior. Thicknesses of the test specimens were selected as 15 mm to prevent the out of plane deformations. The faces of the test specimens in contact with soil were roughened. In the experimental study, test specimens were located upon the soil to simulate the shallow foundation behavior.

The test specimens were located on the sand container that was specially designed for this experimental study. The specially used sand was relocated in the test setup for each test to satisfy the 55% compactness value ($\gamma = 16.6 \text{ kN/m}^3$). The maximum and minimum densities, specific weight (G_s), and gradation of the well graded sand were determined through experiments and presented in Table 2. The internal friction angle of the sand was obtained as 39.0° from the shear box tests conducted on the sand specimens at 55% relative density. This internal friction angle was obtained for the axial stress values changing between 95 and 500 kPa. The gradation curve of the sand is given in Fig. 2. All tests were conducted using totally dry sand samples. For this purpose, the sand was dried in oven before each experiment.

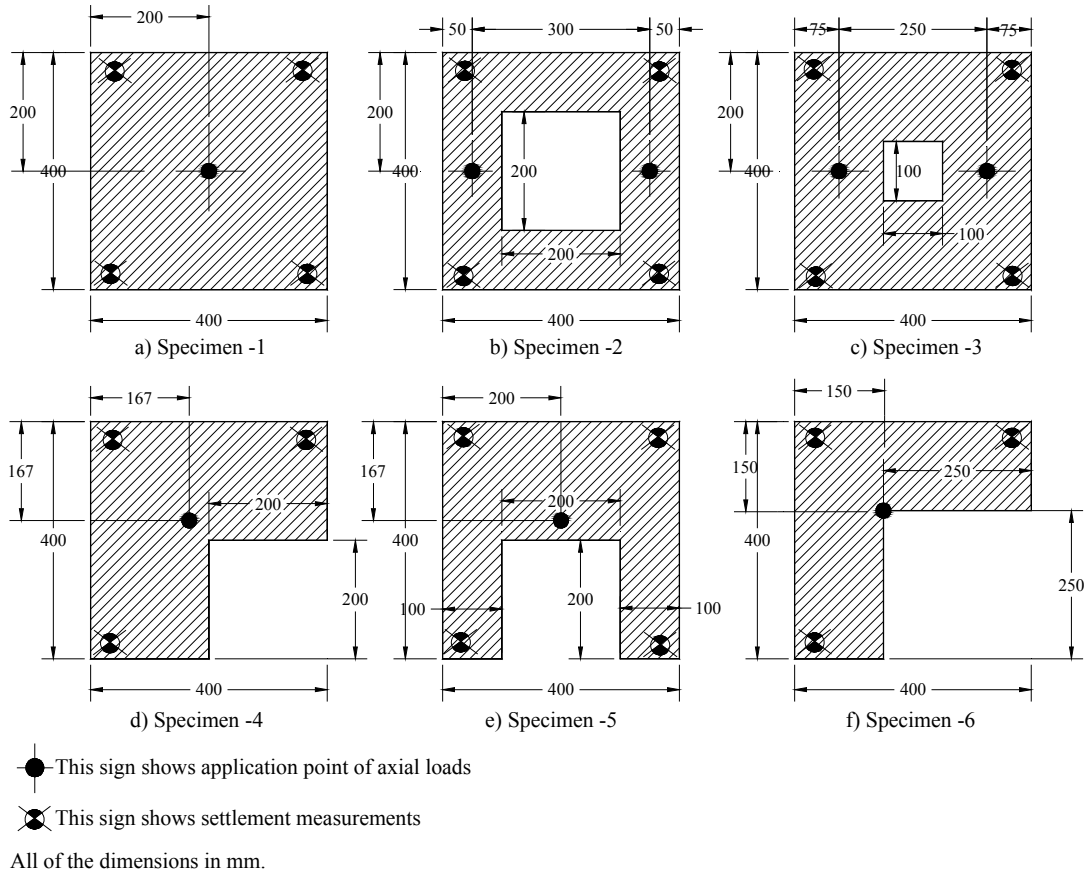


Fig. 1 Geometry of test specimens

Table 1 Property of test specimens

Specimen No.	Definition	Foundation shape
1	Square foundation	
2	Square foundation with large hole	
3	Square foundation with small hole	
4	Large L shaped foundation	
5	U shaped foundation	
6	Small L shaped foundation	

Table 2 Properties of sand

G_s	ρ_{min} (Mg/m ³)	ρ_{max} (Mg/m ³)	e_{min}	e_{max}	D_{10}	D_{50}	C_c	C_u	Fine %
2.71	1.55	1.82	0.48	0.75	0.12	0.62	1.0	7.5	4.9

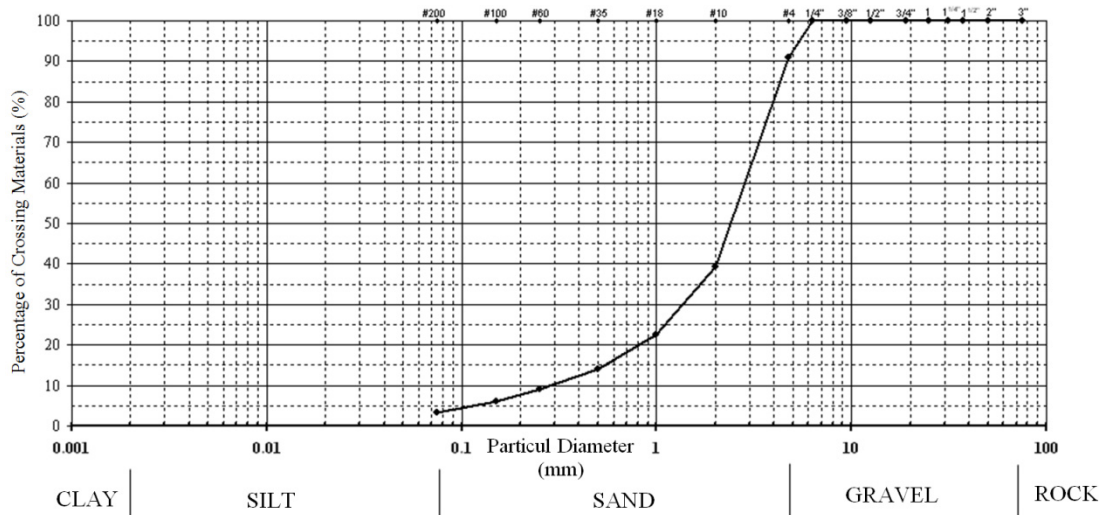


Fig. 2 Particle size distribution of sand

2.2 Test setup

Footing experiments were conducted in a container manufactured using 5 mm thick steel plates with the dimensions of 2000 mm × 2000 mm × 1000 mm. In order to conduct the experiments the specially graded sand was placed in the container at the previously stated relative density and in a dry form. Therefore, the properties of the sand used in the experiments kept constant during all experiments. In order to provide constant water content, internal friction angle and compactness ratio the experiments were conducted with care and after each experiment, sand in the container was refilled. Furthermore, the container was marked at specific intervals of predetermined volumes so that the same amount of sand was filled to obtain identical geotechnical properties. Before conducting each experiment, the sand was dried and weighted before filling it into the container. NPU steel profiles with the dimensions of 140 mm × 140 mm × 4 mm were manufactured as a closed form loading frame. The axial loading was applied using a 300 kN pressure capacity hydraulic jack and the level of axial loading was measured using a 225 kN capacity loading cell. The deformations of test specimens were measured using four vertical linear variable displacement transducers (LVDTs). These vertical deformation measurements were used to obtain the settlement profiles of the footings. Locations of the axial loading points and LVDTs' locations are given in Fig. 1 for all test specimens. All measurements were transferred to the computer using a data logger. The experiments were conducted by tracing the vertical load displacement relationships of the test specimens. Consequently, the effect of shape irregularity on the settlement profile of footings was obtained and interpreted. Test and measurement setup is given in Fig. 3. A photograph of the test setup in the time of an experiment is given in Fig. 4. Loading rate was kept constant during all experiments at 5 N/sec using a hydraulic loading system.

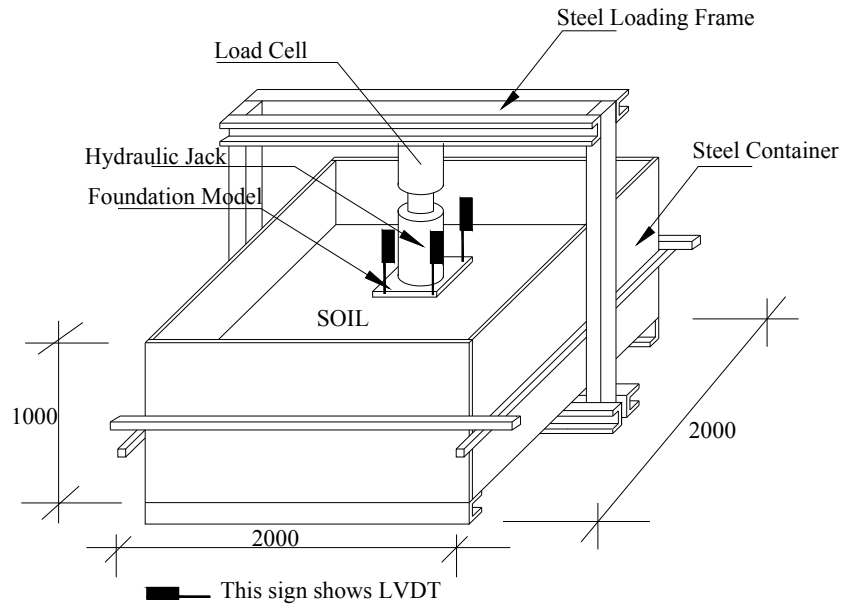


Fig. 3 Test setup and instrumentation



Fig. 4 Photo of test setup before testing

3. Experimental results

3.1 Bearing capacities

All experimental results in terms of maximum axial loads, bearing capacities at 40 mm settlement, settlements in terms of profiles and mean values (calculated by taking the average of all settlement measurements on the footing) are given in Table 3. The measurement of the settlement profiles were taken by using LVDTs (i.e., 3 LVDTs on specimens 4 and 6, 4 LVDTs on other specimens). Measurement points are shown in Fig. 1. The largest axial load was applied to

the reference test specimen – 1 to observe a settlement value of 40 mm. Test specimen – 6 with the smallest footing surface area carried the lowest bearing load with respect to the other test specimens. The L shaped specimen – 6 reached 40 mm mean settlement level under a relatively small axial loading of 10.5 kN. The rectangular specimen-1 carried a 1.83 times larger load than the L shaped specimen – 6 (Table 3). Specimen – 2 with the large square opening, L shaped specimen – 4 and U shaped specimen – 5 have the same contact surface areas. However, these specimens reached the 40 mm mean settlement levels under different axial load levels showing the significance of the location of the opening on the footing behavior. Test specimen – 2 with an opening located at the intersection of two symmetry axes reached an axial load 2% higher than that of the test specimen – 5 with an opening located on one of the symmetry axes. On the other hand, the measured average settlement of the test specimen -2 was higher than that of test specimen – 5 under lower axial load magnitudes. Presence of an opening located at the center of specimens lead to higher settlement ratios due to the higher values of stresses at the center of test specimens. In relation to that the settlement values of specimen 2 with a central opening, were higher than those of specimen 5. A 4% higher bearing capacity was observed in specimen – 2 compared to test specimen – 4, which has an opening located at the corner of the footing. Furthermore, it was observed that the bearing capacity of specimen – 5 with an opening located on one of the symmetry axes was 3% higher than that of test specimen – 4 with an opening located at the corner of the footing.

From the comparison of footings with similar shapes but having different opening areas, it was observed that in terms of bearing capacities, i.e., loads at 40 mm settlement, test specimen – 3 with a small square opening showed a 27% higher performance than test specimen – 2 with a large square opening. Test specimen – 4, L shaped footing with large area, had a 28% higher load than that of test specimen – 6, L shaped footing with small area, at the same settlement level of 40 mm. On the other hand, it should be noted that the comparisons given above are presented in terms of measured loads. The variation of the corresponding stress levels of the considered foundations (Table 3), corresponding to the 40 mm settlement value, is smaller than the variation of the ultimate load levels.

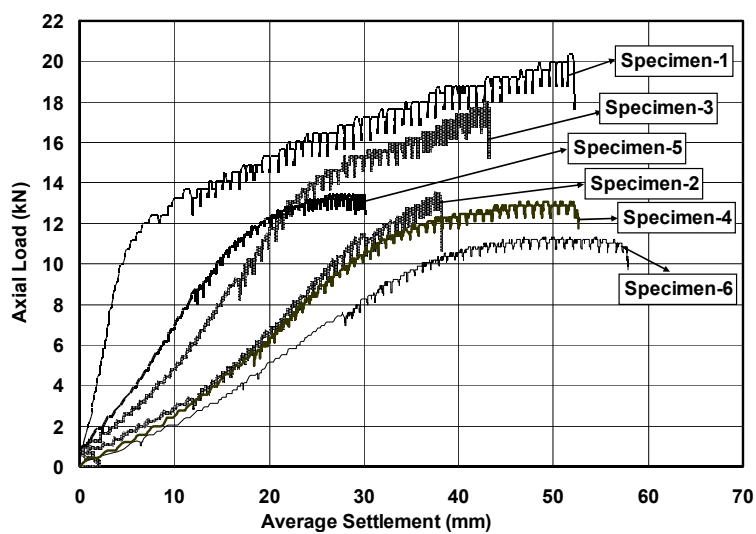


Fig. 5 Axial load vs. average settlement graphs of specimens

Table 3 Experimental results

Spec. No	Description	Maximum axial load (kN)	Bearing capacity* load/stress (kN/kPA)	Settlement profile a maximum load (mm)**				Average *** settlement (mm)
				Right front	Right back	Left front	Left back	
1	Square foundation	20.05	18.77 / 117.31	47.22	54.04	48.21	59.42	52.23
2	Square foundation with big hole	15.06	13.58 / 113.17	32.23	36.94	39.08	43.22	37.87
3	Square foundation with little hole	17.99	17.29 / 115.27	46.63	35.47	48.93	40.90	42.98
4	Big <i>L</i> shaped foundation	13.05	12.99 / 108.25	-----	51.21	48.87	57.76	52.61
5	<i>U</i> shaped foundation	13.42	13.42 / 111.83	35.90	25.81	35.38	26.17	30.80
6	Little <i>L</i> shaped foundation	11.36	10.24 / 105.03	-----	60.23	53.83	59.48	57.85

* Axial loads measured at 40 mm settlement which corresponds to 10% of the foundation width

** Settlement measurement locations are shown in Fig. 1.

*** Average settlements are calculated at maximum axial load level

The mean settlement – axial load relationships of the all test specimens are presented in Fig. 5. As expected, in case of larger openings the test specimens demonstrated lower load capacities at a given settlement value. From the test results it is observed that the largest axial load was applied to the reference square test specimen – 1 to observe a settlement value of 40 mm. In contrary, test specimen – 6 with the lowest surface area showed the lowest axial load performance with respect to the other specimens.

3.2 Settlement profiles

Settlement profiles of the test specimens were measured using the LVDTs, located at the displacement measurement points, shown in Fig. 1. Settlement values of the test specimens, measured at the maximum axial load levels, are given in Table 3. From the investigation of the settlement values, it was observed that the maximum differences among the settlement values of the given model footing were measured in the *L* shaped test specimen – 5. The difference between maximum and minimum settlement levels was calculated to be 39% in the *L* shaped test specimen – 5. Test specimens with largest differential settlements in the descending order are Specimen 3, Specimen 2, Specimen 1, Specimen 4 and Specimen 6, respectively. These differences are 38%, 34%, 26%, 18% and 12% for test specimens Specimen 3, Specimen 2, Specimen 1, Specimen 4 and Specimen 6, respectively.

Differences between the corner settlements of the specimens (which are measured under the axial load level corresponding to a mean settlement level of 40 mm) are smaller than those measured under the maximum axial load level. The smallest settlement differences were observed in *L* shaped specimens – 4 and 6, in contrary, the largest settlement differences were observed in test specimen 2. Average settlement difference of all test specimens was calculated as 7%. This

value is 74% smaller than those obtained at the maximum axial load level. These observations illustrate that the axial load levels larger than the bearing capacities of the test specimens cause the settlement profiles to rapidly deviate from the uniform distribution.

4. Analytical study

4.1 Theoretical calculations with proposed equations in the literature

As stated before, in this study, the bearing capacity (q_o) is defined as the axial load level causing a settlement in the footing corresponding to 10% footing width. As stated by Cerato and Lutenegeger (2006) this approach has no theoretical base. However, it is a value that is easy to remember, close to the soil strains in case of failure, pushes q_o to take a certain and constant value and allows to compare the behavior of footings with different geometries in a similar manner. Consequently, it may be used as a useful practical criterion. The values employed in the widely accepted equations proposed to calculate the bearing capacities of the square, circular and rectangular footings are given in Table 4. The values used in the calculations were measured at the 40 mm mean settlement values. In order to have realistic footing length/width (B) values, the footings were assumed to be in a square form and their side lengths are calculated as the square root of the surface areas of the footings.

Bearing capacities of the test specimens are calculated using the equations proposed by

Table 4 Calculation parameters used for equations

Spec. No.	Description	B (m)	D (m)	L/B	γ (kN/m ³)	ϕ (°)	Load (kN)
1	Square foundation	0.400	0	1	16.8	39	18.77
2	Square foundation with big hole	0.346	0	1	16.8	39	13.58
3	Square foundation with little hole	0.387	0	1	16.8	39	17.29
4	Big L shaped foundation	0.346	0	1	16.8	39	12.99
5	U shaped foundation	0.346	0	1	16.8	39	13.42
6	Little L shaped foundation	0.312	0	1	16.8	39	10.24

Table 5 Comparison of bearing stresses of specimens

No.	Description	Terzaghi (kPa)	Meyerhof (kPa)	Hansen (kPa)	Vesic (kPa)	Experiment q_o^* (kPa)	Shape factor
1	Square foundation	268.02	374.05	134.58	185.97	117.31	0.60**
2	Square foundation with big hole	231.84	323.55	116.41	160.86	113.44	0.67
3	Square foundation with little hole	259.31	361.89	130.21	179.92	115.44	0.61
4	Big L shaped foundation	231.84	323.55	116.41	160.86	108.51	0.64
5	U shaped foundation	231.84	323.55	116.41	160.86	112.10	0.66
6	Little L shaped foundation	209.06	291.76	104.97	145.06	105.19	0.69

* Experimental bearing capacities of specimens were calculated at 40 mm settlement which corresponds to 10% of the foundation width.

** According to Vesic (1975)

Terzaghi (1943), Meyerhof (1951, 1963), Hansen (1970), Vesic (1975) and presented in Table 5. Consequently, the bearing capacities obtained using experimental study and those obtained using the stated equations are compared. From the comparisons, it is observed that the bearing capacities calculated using the equation proposed by Hansen (1970) generally yielded the closest results obtained from the experimental study.

Note that an effort was also undertaken to estimate the “equivalent” shape factors for the irregularly shaped foundations considered in this study. For a fair comparison, equivalent square footing widths tabulated in Table 4 were used along with the experimental bearing capacities given in Table 5 to calculate the shape factors. For the square foundation, a shape factor of 0.60, as suggested by Vesic (1975) was employed. As tabulated in table 5, the results indicate only a modest amount of variation of the shape factor for the footings considered herein. As expected, the shapes that were highly modified from the square one, i.e., the square foundation with the big hole and the little *L* shaped foundation have the highest change from the reference value of 0.60. However, the deviations do not exceed about 15% even for these footings.

4.2 Finite element model

The PLAXIS 3D Foundation software which is capable of performing 3 dimensional analyses was used in this study. PLAXIS 3D Foundation is finite element software which is useful to obtain 3 dimensional finite element solutions of geotechnical problems. This software has been used to analyze problems related to shoreline structures, raft foundations, piled raft foundations and sheet piles (Brinkgreve and Broere 2004). In this paper, PLAXIS 3D Foundation version 1.5 is used.

In the software, there are several soil modeling options such as; linear-elastic, Mohr Coulomb and Hardening. Hardening soil model is more realistic modeling capabilities of pressure under foundations with respect to other soil models (Brinkgreve and Broere 2004). Accordingly, the Hardening soil model is used in this paper. The unit weight of the soil is taken as 16.8 kN/m³. Modulus of elasticity *E*, effective stress friction angle ϕ and dilation ψ variables were entered to software. Cohesion is assumed to be zero ($c = 0$) due to the results of the direct shear tests and zero clay content in the soil used in the experiments.

Firstly, geometry of the model was constructed in the software. The steel container in the dimensions of 2000 × 2000 × 1000 mm was modeled. Then the shape of the soil model was modeled. Consequently, the considered footing was modeled on the soil surface. Then the material properties of soil and footing were defined. The rigid surface of the sand container was modeled by assigning “line fixity” to the four edges of soil model. Next, the loading was defined at the point of interest. The loadings were defined vertically at the center of gravities of the constructed models. Finally, the model was meshed with three dimensional finite elements. Next step was the solution procedure. For the solution, a staged construction strategy was employed. First, the “initial phase” which is the condition of the footing before placed on the soil. Then, “Phase 1” was defined as the position of the footing on the soil and “Phase 2” was defined to activate the loading and starting the solution procedure.

In the simulation procedure, sensitivity analyses were conducted by increasing the number of elements and then the number of elements was decided according to the results from these sensitivity analyses. In the sensitivity analyses, numbers of elements were increased until obtaining a model which leads to a negligible difference in the displacement value of the center of the footing from that of the next model with higher number of elements.

From the finite element analyses conducted using PLAXIS 3D Foundation finite element

software, stress distributions in the soil and settlement profiles at the base of the footing were obtained. In addition, the mean settlement – axial load and settlement – axial load relationships were also obtained from the analyses for comparative purposes. Stress distributions obtained from the finite element analyses are presented in Fig. 6. In addition, at the bottom right corners of the stress distributions, stress distributions at the sides of the foundations are given in a close up view and the A-A sections of the settlement profiles are indicated in Fig. 6. Settlement values obtained, using the A-A section cuts, from the finite element analyses are given in Fig. 7. In the finite element simulations, in order to simulate the boundary conditions of the steel container, the displacement of the nodes at the outer surface of the sand volume was fixed in three directions.

5. Comparison of experimental and analytical results

The load – settlement relationships obtained from the analyses conducted using the PLAXIS finite element software were comparatively plotted with those obtained from the experimental study and presented in Fig. 8. The load – mean settlement relationships of the test specimens were obtained using the settlement measurements taken from the corners of the test specimens via LVDTs. In addition, stresses at the points which are used to calculate the mean settlement profiles in the experimental study are obtained from the finite element analyses results and comparatively given with those of the experimental study (Table 6). From the comparison of experimental and analytical stress values, it is observed that the ratio of these stresses varies between 0.99 and 1.15. The smallest difference between analytical and experimental stresses (1%) is calculated for test specimen – 2. On the other hand the greatest difference between the experimental and analytical stress levels (15%) is calculated for test specimen – 5.

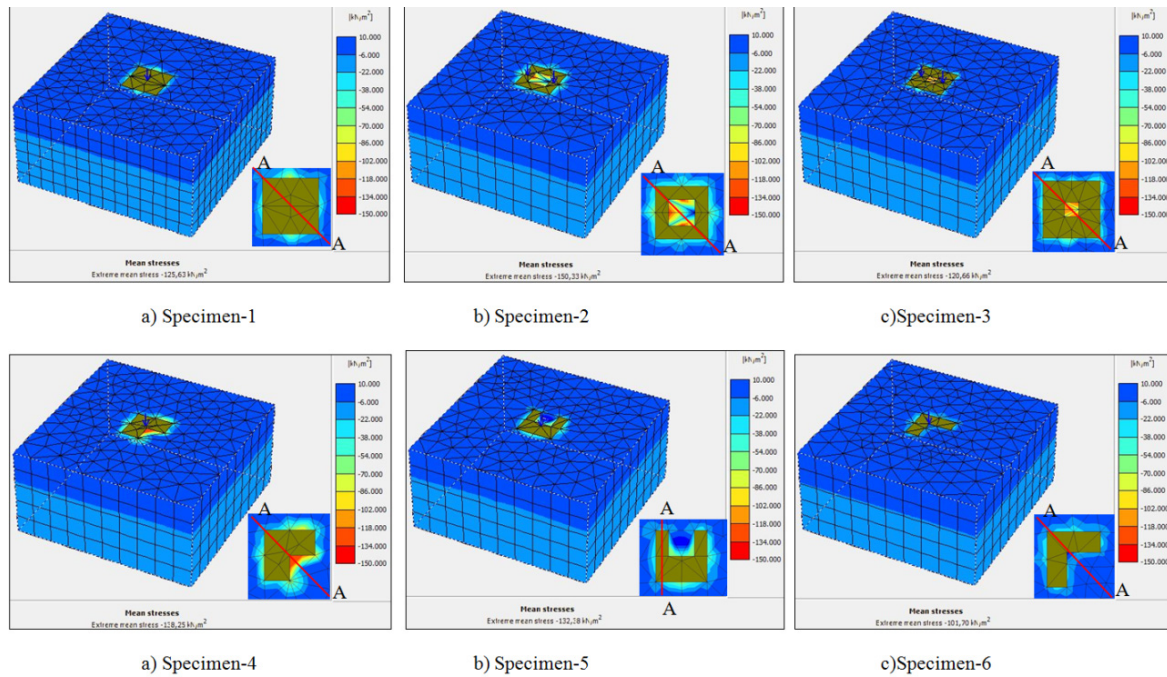


Fig. 6 Stress distributions of specimens

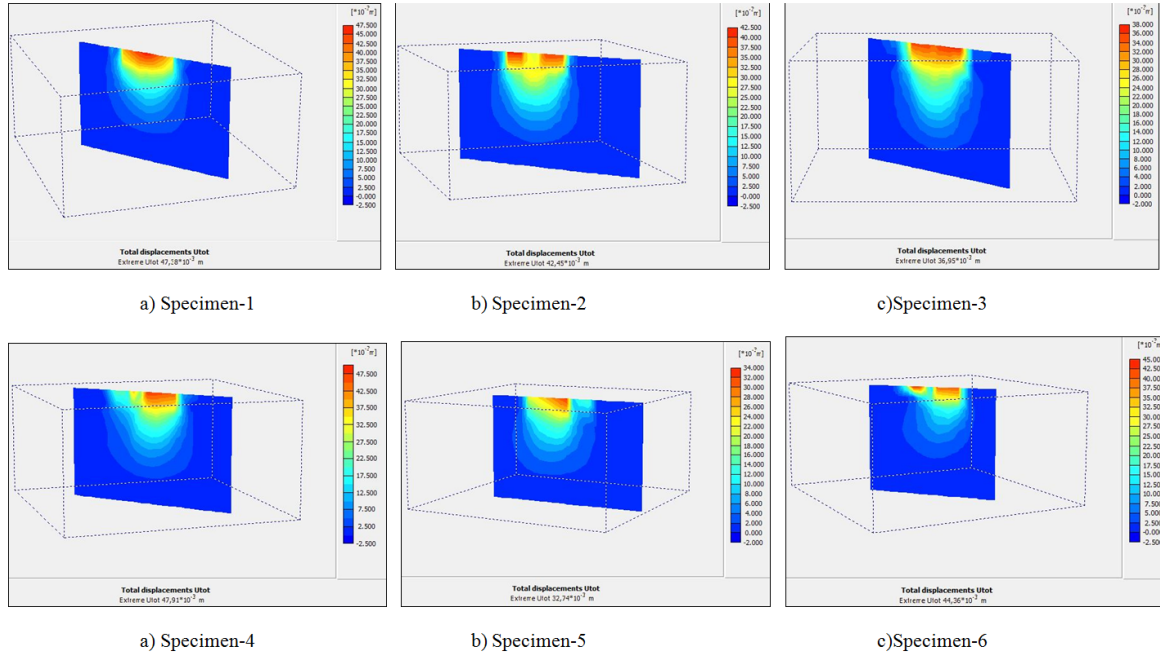


Fig. 7 Displacement profiles of specimens at Section A-A

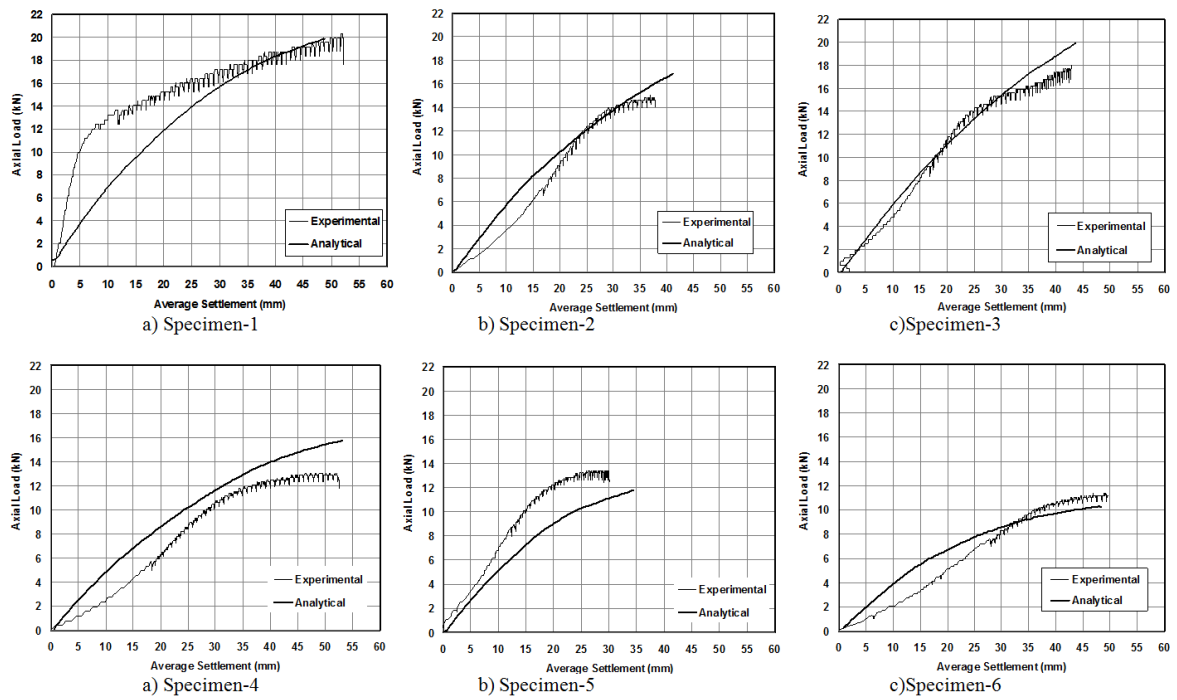


Fig. 8 Comparison of analytical and experimental settlement-load curves of specimens

Table 6 Comparison of experimental and analytical stress values of specimens

Location*	Specimen No.											
	1		2		3		4		5		6	
	E***	A****	E	A	E	A	E	A	E	A	E	A
Right Front	119.77	121.31	118.17	116.17	103.95	114.87	105.26	113.67	105.25	88.67	106.50	99.38
Right Back	117.27	121.31	118.22	115.33	109.97	114.80	103.66	116.42	93.50	83.50	103.09	100.51
Left Front	119.90	120.56	112.84	115.08	107.94	115.00	-----	-----	103.67	89.17	-----	-----
Left Back	112.42	120.69	106.25	115.75	110.04	114.87	100.56	115.25	93.67	83.50	108.15	100.92
Average**	117.34	120.69	113.87	115.58	107.98	114.88	103.16	115.11	99.02	86.21	105.91	100.27

* Stress location that were made a comparison between experimental and analytical

** Average results of stresses

*** Experimental

**** Analytical

Settlement and axial load values of the tested specimens obtained from the finite element analyses and experimental study are comparatively given in Table 7. In the table, maximum settlement and axial load values are presented together with the corresponding ratios of the experimental and finite element analyses results. The largest difference between experimental and analytical settlement values of 16% is calculated for test specimen – 6 and the smallest difference of 1% is calculated for test specimen – 4.

The largest difference between experimental and analytical axial loads (38%) was calculated for test specimen – 4 and the smallest difference of 1% is calculated for test specimen –1. From the results, it is observed that the settlement values obtained using analytical procedures are reasonably close to the experimental values with respect to the corresponding axial load values.

However, the finite element model generally fails to capture the exact nonlinear shape of the load-settlement curve, which would result in erroneous predictions of behavior especially at settlements of small magnitude. This is most likely due to the discrepancy of the modeled and

Table 7 Comparison of analytical and experimental settlement-axial load values

Spec. No	Settlement (mm)			Axial Load (kN)		
	Analytical	Experimental	Ratio*	Analytical	Experimental	Ratio*
1	48.83	52.23	0.93	20.00	20.05	1.00
2	41.15	37.87	1.09	18.00	15.06	1.20
3	43.63	42.98	1.02	19.89	17.99	1.11
4	53.14	52.61	1.01	18.00	13.05	1.38
5	34.39	30.80	1.12	15.00	13.42	1.12
6	48.37	57.85	0.84	10.28	11.36	0.90

* Ratio of analytical to experimental values

observed values of soil moduli at small strains, which is out of the scope of this study. Therefore, it is concluded that the general settlement – axial load behavior calculated using the PLAXIS 3D Foundation software offers a useful acceptable solution to the design engineers during the design process, especially for bearing capacity calculations.

6. Conclusions

In this paper, bearing capacities and settlement profiles of irregularly shaped footings located on sand have been experimentally and analytically investigated under the effect of axial loading. The main variable considered in the paper was the geometry of the footings. Six footings with different geometries and dimensions were tested under the effect of axial loads applied from the center of gravities of the footings. Consequently, the effect of footing shape on the variation of the bearing capacities, stress distributions and settlement profiles of the footings on sand have been investigated. The three dimensional finite element analyses of the tested specimens were conducted using the PLAXIS 3D software. Using the results of experimental and finite element analyses an efficient analytical model was proposed to be used by foundation design engineers. The conclusions drawn from the study are given below.

From the experimental study it was observed that, as expected, the best performance in terms of bearing capacities was given by the square reference test specimen – 1. The bearing capacity, of the test specimen – 1, which is defined to be the applied pressure at a settlement of 10% of the foundation width, was 12% larger than the L shaped test specimen – 6. In terms of bearing capacities, the tested specimens with openings located at the center of the footing gave relatively good performances following the reference test specimen – 1. The bearing capacities obtained from the tests of L shaped specimens are lower than those of the other test specimens. Specimen – 2 with the large square opening, L shaped specimen – 4 and U shaped specimen – 5 all have the same contact surface areas. However, these specimens have different bearing capacities showing the significance of opening location on the footing behavior under axial loads. In terms of load bearing capacities, test specimen – 2 with an opening located at the intersection of two symmetry axes showed about 2% and 4% better performances than test specimen – 5 with an opening located on one of the symmetry axes and test specimen – 4 with an opening located at the corner of the footing, respectively. Furthermore, it was observed that the performance of test specimen – 5 with an opening located on one of the symmetry axes showed 3% better performance than test specimen – 4 with an opening located at the corner of the footing. The observations obtained from the experimental study indicate that if an opening is necessary in the footing, this opening should be placed at the center or at least at one of the symmetry axes of the footing. It was also observed that an increase at the area of the opening generally decreases the bearing capacity. This issue can be important for the design of footings on marginal soils, where the architecturally required opening size must be limited due to geotechnical considerations.

From the stress distributions obtained using the finite element analyses, it is observed that the distribution of stress varies with the location of the opening. Stress concentrations are observed in the vicinity of openings of test specimens – 3, 2, 4 and 6. During the design process of such type of footings, stress concentrations should be accounted for.

From the settlement values measured at the corners of the considered test specimens and from the settlement profiles obtained using the finite element model, it was observed that the best performance was displayed by square shaped test specimen – 1. The settlement profile of the

square test specimen was measured to be quite uniform. In terms of the settlements progressing with increasing loads, the worst performance was displayed by the U-shaped test specimen – 5. The settlement difference between the corners of the U shaped specimen -5 which are close and far from the opening, respectively, was measured as 13%. The varying settlement profile with the area of the opening and with the distance to opening indicated that the different settlements should be carefully considered for this shape.

The three dimensional finite element analyses of the tested specimens were conducted using the PLAXIS 3D software to obtain the bearing capacities of the tested specimens and settlement –load relationships of the tested specimens. From the analyses results, it was observed that the load – settlement relationships obtained until 40 mm settlement generally yield accurate results which are in good agreement with the experimental results. Also, it was observed that the finite element models constructed using the PLAXIS 3D software is reasonably accurate and usable for design engineers especially for bearing capacity considerations.

Acknowledgments

The authors gratefully acknowledge the financial assistance of the Turkish Academy of Sciences, Young Scientist Award program (GEBIP) and Feyzi AKKAYA Scientific Activates Supporting Fund (FABED) Young Investigator Research Award.

References

- Brinkgreve, R.B.J. and Broere, W. (2004), *Plaxis 3D Foundation Manual*, Balkema Publishers, Delft University of Technology & Plaxis B.V., The Netherlands, pp. 7-10.
- Cerato, A.B. and Lutenegeger, A.J. (2006), “Bearing capacity of square and circular footings on a finite layer of granular soil underlying by a rigid base”, *J. Geotech. Geoenviron. Eng., ASCE*, 1496-1501.
- Chen, W.F. and McCarron, W.O. (1991), *Foundation engineering handbook*; (Ed. H.-Y. Fang), New York, NY, USA, Van Nostrand Reinhold, pp. 144-165.
- De Beer, E.E. (1970), “Experimental determination of the shape factors and the bearing capacity factors of sand”, *Geotechnique*, **20**(4), 387-411.
- Dixit, M.S. and Patil, K.A. (2013), “Experimental estimate of N_γ values and corresponding settlements for square footings on finite layer of sand”, *Geomech. Eng., Int. J.*, **5**(4), 363-377.
- Hansen, J.B. (1970), “A revised and extended formula for bearing capacity”, Bulletin No. 28; Danish Geotechnical Institute, Lyngby, Denmark.
- Lyamin, A.V., Salgado, R., Sloan, S.W. and Prezzi, M. (2007), “Two and three-dimensional bearing capacity of footings in sand”, *Geotechnique*, **57**(8), 647-662.
- Mabrouki, A., Benmeddour, D. and Mellas, M. (2009), “Numerical study of bearing capacity for a circular footing”, *Australian Geomech.*, **44**(1), 91-100.
- Mabrouki, A., Benmeddour, D., Frank, R. and Mellas, M. (2010), “Numerical study of the bearing capacity for two interfering strip footings on sands”, *Comput. Geotech.*, **37**(4), 431-439.
- Meyerhof, G.G. (1951), “The ultimate bearing capacity of foundations”, *Geotechnique*, **2**(4), 301-332.
- Meyerhof, G.G. (1963), “Some recent research on bearing capacity of foundations”, *Can. Geotech. J.*, **1**(1), 16-26.
- Mohamed, F.M.O., Vanapalli, S.K. and Saatcioglu, M. (2013), “Generalized Schmertmann Equation for settlement estimation of shallow footings in saturated and unsaturated sands”, *Geomech. Eng., Int. J.*, **5**(4), 343-362.
- Naderi, E. and Hataf, N. (2014), “Model testing and numerical investigation of interference effect of closely

- spaced ring and circular footings on reinforced sand”, *Geotext. Geomembr.*, **42**(3), 191-200.
- Prandtl, L. (1921), “Über die eindringungsfestigkeit plastischer baustoffe und die festigkeit von schneiden”, *Math. Mech.*, **1**(1), 15-20.
- Reissner, H. (1924), “Zemerddruck problem”, *Proceeding of the 1st International Conference on Applied Mechanics*, (C.B. Biezeno and J.G. Burgers Eds.), *J. Walkman Jr.*, Delft, Netherlands, pp. 295-311.
- Shahin, M.A. and Cheung, E.M. (2011), “Stochastic design charts for bearing capacity of strip footings”, *Geomech. Eng., Int. J.*, **3**(2), 153-167.
- Tani, K. and Craig, W.H. (1995), “Bearing capacity of circular foundations on soft clay of strength increasing with depth”, *Soils Found.*, **35**(4), 21-35.
- Terzaghi, K. (1943), *Theoretical Soil Mechanics*, Wiley, New York, NY, USA.
- Vesic, A.S. (1975), “Bearing capacity of shallow foundations”, In: *Foundation Engineering Handbook* (Eds. Winterkorn & Fang), Van Nostrand Reinhold, New York, NY, USA, pp. 121-147.
- Zhu, M. and Michalowski, R.L. (2005), “Shape factors for limit loads on square and rectangular footings”, *J. Geotech. Geoenviron. Eng.*, **131**(2), 223-231.